Acta Cryst B
STRUCTURAL SCIENCE
CRYSTAL ENGINEERING
MATERIALS
ISSN 2052-5206

TAAM: a reliable and user friendly tool for hydrogen-atom location using routine X-ray diffraction data

Kunal Kumar Jha, Barbara Gruza, Prashant Kumar, Michal Leszek Chodkiewicz* and Paulina Maria Dominiak*

Biological and Chemical Research Centre, Department of Chemistry, University of Warsaw, ul. Żwirki i Wigury 101, Warszawa, 02-089, Poland. *Correspondence e-mail: mchodkiewicz@chem.uw.edu.pl, pdomin@chem.uw.edu.pl

Received 5 November 2019
Accepted 2 March 2020

Edited by P. Macchi, University of Bern, Switzerland

Keywords: IAM; TAAM; *DiSCaMB*; HAR; aspherical scattering factors; quantum crystallography; structure refinement.

Supporting information: this article has supporting information at journals.iucr.org/b

Hydrogen is present in almost all of the molecules in living things. It is very reactive and forms bonds with most of the elements, terminating their valences and enhancing their chemistry. X-ray diffraction is the most common method for structure determination. It depends on scattering of X-rays from electron density, which means the single electron of hydrogen is difficult to detect. Generally, neutron diffraction data are used to determine the accurate position of hydrogen atoms. However, the requirement for good quality single crystals, costly maintenance and the limited number of neutron diffraction facilities means that these kind of results are rarely available. Here it is shown that the use of Transferable Aspherical Atom Model (TAAM) instead of Independent Atom Model (IAM) in routine structure refinement with X-ray data is another possible solution which largely improves the precision and accuracy of X—H bond lengths and makes them comparable to averaged neutron bond lengths. TAAM, built from a pseudoatom databank, was used to determine the X—H bond lengths on 75 data sets for organic molecule crystals. TAAM parametrizations available in the modified University of Buffalo Databank (UBDB) of pseudoatoms applied through the *DiSCaMB* software library were used. The averaged bond lengths determined by TAAM refinements with X-ray diffraction data of atomic resolution ($d_{\min} \leq 0.83$ Å) showed very good agreement with neutron data, mostly within one single sample standard deviation, much like Hirshfeld atom refinement (HAR). Atomic displacements for both hydrogen and non-hydrogen atoms obtained from the refinements systematically differed from IAM results. Overall TAAM gave better fits to experimental data of standard resolution compared to IAM. The research was accompanied with development of software aimed at providing user-friendly tools to use aspherical atom models in refinement of organic molecules at speeds comparable to routine refinements based on spherical atom model.

1. Introduction

Hydrogen is the most abundant element in the universe. It is present in almost all molecules in living things (Emsley, 2011; Vladilo & Hassanali, 2018). It is highly reactive. It forms bonds with most elements, terminating their valences and enhancing the chemistry of those elements. Hydrogen bonding is responsible for the unique solvent properties of water, holding the two complementary strands of DNA together, the 3-D folding of proteins in enzymes and antibodies, binding of ligands to receptors and many other things. Hydrogen plays a significant role in many catalytic reactions both in biological systems and in small molecule chemistry (Taylor & Jacobsen, 2006; Doyle & Jacobsen, 2007; Głowacki *et al.*, 2013; Belkova *et al.*, 2016). Understanding of the catalytic mechanisms of enzymes, the mechanism of protein folding and ligand–

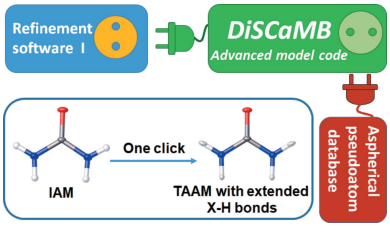

receptor complex formation demands accurate and precise determination of the position of the hydrogen atoms (Agback & Agback, 2018; Chen *et al.*, 2016).

X-ray diffraction is the most commonly used method for chemical structure determination. This method depends on scattering of X-rays by the electron density, which is relatively low for hydrogen atoms; therefore, hydrogens are difficult to locate (Müller *et al.*, 2006). To overcome this, neutron diffraction is used to determine the accurate position of hydrogen atoms, utilizing the fact that the neutron scattering length for hydrogen atoms is comparable to heavier elements. Most of the neutron diffraction experiments demand large single crystals (>1 mm^3). Recent advancements in technology have made it possible to collect neutron data on smaller crystals (<1 mm^3); however, the costly maintenance of neutron sources and the limited number of neutron diffraction facilities are significant bottlenecks for these kind of studies.

In general, routine diffraction data are modeled using an Independent Atom Model (IAM) which is based on individual atom contributions. The atoms in IAM are represented by spherically averaged electron density distributions obtained from quantum chemistry calculations for isolated atoms in their ground state (Coppens, 1997). However, the electron density of an isolated hydrogen atom is significantly different from the one of a bonded hydrogen atom and the scattering factor obtained from IAM leads to meaningless bond lengths and other unrealistic properties (Stalke, 2012). The lack of core electrons in the hydrogen atom and polarization of its electron density towards the bonding regions (*i.e.* along the X—H bond, where X is any non-hydrogen atom), cause the X—H bond lengths determined for hydrogen atoms by IAM to be much shorter than expected. Additionally, the electron density in the vicinity of the proton in bonded hydrogen atoms is contracted compared to the isolated atom causing isotropic displacement parameters to be abnormally low (Stewart *et al.*, 1965). Improvements to scattering factors for hydrogen, based on the *ab initio* electron density of the hydrogen molecule were proposed by Stewart, Davidson and Simpson (1965). The best spherical density model for bonded hydrogen recommended by them (SDS), along with IAM for other atoms, was used until now in most of the routine X-ray structure determination protocols (Wilson & Geist, 1993), which allow refinements to obtain more reliable isotropic displacement parameters for hydrogen atoms, but still lead to X—H bond lengths ≃20% shorter than the values obtained from neutron diffraction data (Stewart *et al.*, 1965). Later it was noted that high-order refinement (d_{min} < 0.7 Å) which improves the accuracy of atomic positions (Ruysink & Vos, 1974; Coppens, 1968) also shows a considerable improvement in the X—H bond lengths (Hope & Ottersen, 1978; Almlöf & Ottersen, 1979). A further attempt by Stewart and co-workers was based on a fixed multipole expansion for a bonded hydrogen atom (*i.e.* polarized hydrogen atom) (Stewart *et al.*, 1975). This model has largely improved the X—H bond lengths and has been successfully applied to a few systems (Roversi *et al.*, 1996; Destro *et al.*, 1988, 2000; Madsen *et al.*, 2004), but it was not yet as efficient or accurate to match the mean X—H bond lengths from neutron data. There are few other non-empirical methods available, such as extension of the X—H bond (Madsen *et al.*, 2004; Overgaard *et al.*, 2009), a combined approach, in which the high- and low-order refinement for non-hydrogen atoms and hydrogen atoms, respectively, along with the subsequent extension of the X—H bond is utilized to match the mean bond length values obtained from neutron data (Hoser *et al.*, 2009).

It has been noted that the values of electron density parameters obtained from multipolar refinements based on Hansen and Coppens (1978) formalism are almost identical for atoms in a similar chemical environment (Brock *et al.*, 1991). Therefore, a number of databanks were developed for different types of so-called transferable aspherical atoms (pseudoatoms) and the databanks were applied to create an electron density model called the Transferable Aspherical Atom Model (TAAM). The most common databanks are: ELMAM2 (Zarychta *et al.*, 2007; Domagała *et al.*, 2012; Nassour *et al.*, 2017), Invariom (Dittrich *et al.*, 2004, 2005, 2006, 2013) and UBDB (Volkov *et al.*, 2007; Dominiak *et al.*, 2007; Jarzembska & Dominiak, 2012; Kumar *et al.*, 2019). In TAAM, instead of refining the parameters of atomic electron density, they are simply constrained to values typical for the corresponding atom type. The use of TAAM instead of IAM in the crystal structure refinement procedure with the standard diffraction [$d_{min} \leq 0.83$ Å, $\sin\theta/\lambda = 0.6$ $Å^{-1}$ recommended in the crystallographic journals (Spek, 2003, 2020)] has largely improved the X—H bond lengths which became comparable to corresponding averaged neutron lengths (Dittrich *et al.*, 2005, 2006; Bendeif & Jelsch, 2007; Domagała *et al.*, 2011; Dadda *et al.*, 2012; Ahmed *et al.*, 2011; Bąk *et al.*, 2011; Dittrich *et al.*, 2017). Other refinement parameters, such as reliability factor (R_f) and residual densities, are also improved (Dittrich *et al.*, 2006; Volkov *et al.*, 2004; Pichon-Pesme *et al.*, 2004; Bąk *et al.*, 2011). However, these methods were limited to specific users and uses due to the complexity of their application. Despite the dedicated work of the software developers of *MoPro* (Domagała *et al.*, 2012), *Invariom Tools* (Dittrich *et al.*, 2004, 2013), *LSDB* (Volkov *et al.*, 2004), *XD* (Volkov *et al.*, 2006), *Jana2006* (Petříček *et al.*, 2014) and other highly specialized programs, TAAM refinement still required a high level of expertise to be reliably performed.

A new technique called Hirshfeld Atom Refinement (HAR), which is based on tailor-made aspherical atomic electron densities extracted from a crystal-field–embedded quantum-chemical electron density using Hirshfeld's scheme (Hirshfeld, 1977; Jayatilaka & Dittrich, 2008; Capelli, Bürgi, Dittrich *et al.*, 2014; Woińska *et al.*, 2014), was introduced. The general applicability of HAR in estimating the X—H bond lengths in small molecules was shown by Woinska *et al.* (2016) where the accuracy and precision were comparable to mean averaged neutron bond lengths. The HAR method was implemented in the *Tonto* program (Jayatilaka & Grimwood, 2003) and later interfaced with *Olex2* (Fugel *et al.*, 2018). Coupling HAR with the databases of extremely localized molecular orbitals [ELMO-DB; Meyer *et al.* (2016), Meyer & Genoni (2018)] reduced the time of computing the wave-

function for HAR without affecting the accuracy or the precision of the refinements (Malaspina *et al.*, 2019). However, the computational cost of HARs and even of ELMO-DB HARs (when very large macromolecules are investigated) are still much higher compared to TAAM refinements. Another recent approach is the use of Bond Oriented Deformation Density (BODD) and Lone Pair Electron Density (LONE) via a tool called IDEAL (Lübben *et al.*, 2019). This approach refines data as fast as IAM alone but does not reach the same sophistication in representing electron density as TAAM (including Invarioms) or HAR (Lübben *et al.*, 2019).

While TAAM refinement is computationally more efficient, previous implementations of this method have not been used by a wide range of users who are not its developers. In this work, the applicability of TAAM in determining the X—H position with comparable accuracy and precision to neutron data was reinvestigated with the same 75 organic crystal data sets used by Woinska *et al.* (2016). We focused our efforts on making TAAM-based refinements user friendly and also to provide a general software solution for determination of X—H bond lengths with high accuracy and precision for routine X-ray structure determination at $d_{\min} \leq 0.83$ Å. For this a new software implementation called *DiSCaMB* (Densities in Structural Chemistry and Molecular Biology) was developed to facilitate integration of the aspherical atom model into a wide range of refinement programs commonly used in X-ray crystallography for small and macromolecules (Chodkiewicz *et al.*, 2018). Here, the structures were modeled and refined using the TAAM-equipped library in *DiSCaMB* integrated with *Olex2* (Dolomanov *et al.*, 2009). The X—H bond lengths obtained from this were categorized and compared with the averaged neutron lengths (Allen & Bruno, 2010). A total of 24 types of X—H bonds were categorized for these 75 structures based on the hybridization and surrounding atoms of attached C, N, O, P atoms. Additionally O—H bonds in water molecules trapped in these structures were also included. Two sets of refinement were performed and related statistical comparison between the different models such as IAM, HAR (Woińska *et al.*, 2016) and TAAM were made, *i.e* at both the maximum resolution as obtained from the deposited structures and also at routine standard resolution of $d_{\min}$ = 0.8 Å. Additionally, anisotropic refinements of hydrogen-atom displacements were performed using TAAM.

2. Methodology

2.1. Implementation

The *DiSCaMB* library, capable of calculating scattering factors for Hansen–Coppens multipole model (Chodkiewicz *et al.*, 2018; Gildea *et al.*, 2011), was extended to support TAAM by adding the capability to recognize atom types and handle TAAM parameters from a pseudoatom databank. A new format for a databank was developed and the UBDB2018 databank (Kumar *et al.*, 2019) was translated to the new format. The details of the atom-typing algorithm implementation and the new databank format will be published elsewhere.

For the purpose of this study, a locally modified version of *Olex2* (version 1.2) (Dolomanov *et al.*, 2009) was used for the refinements. Among others, it incorporates the TAAM X-ray scattering factors available in the *DiSCaMB* library into the *olex2.refine* module.

The newly released version 1.3 of *Olex2* permits the use of non-spherical atomic form factors provided via a text file (Midgley *et al.*, 2019). Files for the kind of TAAM parameterization applied in this work can be generated with a program called *discamb2tsc* (available from http://4xeden.uw.edu.pl) and used for refinements with a publicly available version of *Olex2* (Dolomanov *et al.*, 2009). Results obtained with both implementations [(1) locally modified version of *Olex2* version 1.2 and (2) *discamb2tsc* + *Olex2* version 1.3] are essentially the same.

2.2. Crystal structure data sets

The starting geometries for 81 organic molecule crystal data sets were taken from the supplementary material of Woinska *et al.* (2016), where the selection criteria for these structures are described. The reflection data sets were taken directly from original literature or Cambridge Structural Database (Groom *et al.*, 2016). In four cases (Nos. 9, 17, 43 and 77 in Table S1) the data were not publicly available. The reflection data were used for refinements as they were published, without any omission of reflections except for additional comparative analyses mentioned in Section 3.4 and for data set Nos 19, 27, 42 and 75. For the last four data sets, reflection omission was necessary to achieve refinement convergence.

2.3. IAM refinements

Structures were refined using the default IAM framework (Wilson & Geist, 1993) with *olex2.refine* from *Olex2* (v1.2) using the diffraction data at maximum resolution and truncated at $d_{\min}$ = 0.8 Å. Hydrogen atoms were modeled with the SDS bonded hydrogen model and refined with isotropic displacement parameters, freely without any restraints or constraints. The averaged X—H bond lengths obtained were compared with the reported IAM results (Woińska *et al.*, 2016) obtained using *SHELXL* (Sheldrick, 2015).

2.4. TAAM refinement

The structures obtained from IAM were further refined with *olex2.refine* integrated with TAAM. For the 13 missing atom types in the modified UBDB2018 databank (Kumar *et al.*, 2019), the new atom types were defined and the corresponding aspherical parameters for atomic form factors were calculated. The procedure for addition of new atom types have been discussed elsewhere (Dominiak *et al.*, 2007; Kumar *et al.*, 2019). In one case (No. 3 in Table S1) there were insufficient model molecules available in the CSD representing the three atom-type missing according to the currently used atom-typing algorithm in the UBDB and in another case (No. 72 in Table S1) the molecule contained an exceptionally strong

intramolecular hydrogen bond which could not be accounted for within the current atom-typing algorithm (Woińska *et al.*, 2014). Out of the 81 structures, 75 are subjected to further analysis.

2.5. HAR data

The HAR data were taken as published in the supplementary material of Woinska *et al.* (2016).

2.6. Statistical analysis

All the statistical analyses were performed following the procedures described by Woinska *et al.* (2016).

3. Results and discussions

3.1. Comparison of high-resolution X-ray IAM and TAAM refinements with neutron data for averaged *X*—H bond lengths

The initial IAM-based refinement comparison between the reported (Woińska *et al.*, 2016) and *olex2.refine* results showed that the *X*—H bond length were in very good agreement (Fig. S1), so there was no significant difference introduced by the refinement software. The statistical comparison of the different types of *X*—H bonds obtained from X-ray data after IAM, HAR (Woińska *et al.*, 2016) and TAAM refinements (with isotropic model of hydrogen-atom displacements) at 0.8 Å and also the maximum reported resolution were performed with neutron data as reference, Fig. 1. Further statistical details are given in the SI (Table S1 and S2).

There is a significant *X*—H bond extension in TAAM refinement compared to IAM which caused the *X*—H bond lengths to approach the mean neutron values [Fig. 1(*a*)]. The differences between the mean bond lengths from the X-ray TAAM and neutron data were very low, typically one TAAM sample standard deviation (SSD) for all bond types. This error was reduced to less than one TAAM SSD for bond types with at least 30 representatives (Table S2). Mean bond lengths from IAM usually had a deviation of more than five IAM SSDs compared to neutron and TAAM lengths [Fig. 1(*a*)]. The difference in individual bond-type lengths from TAAM varies from 0.001 Å to 0.05 Å compared to neutron bond lengths. The averaged difference between TAAM and neutron mean lengths for all bond types was 0.025 Å which is comparable to the neutron SSDs (0.017 Å) averaged over all bond types. On the other hand, the mean IAM bond lengths were shorter by

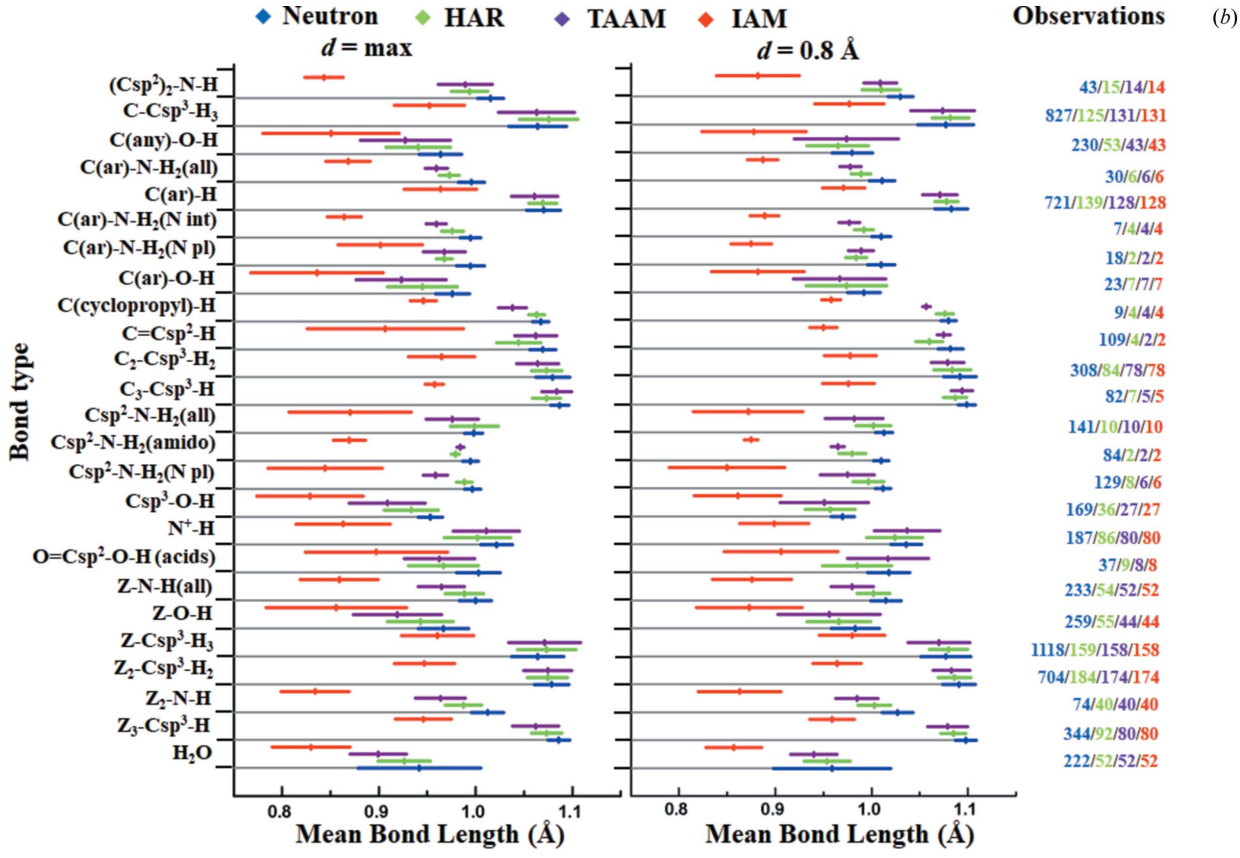

Figure 1
Comparison of the *X*—H bond lengths from X-ray and neutron data refinement at (*a*) maximum and (*b*) 0.8 Å resolution for the selected 75 structures. Hydrogen atoms were refined with isotropic displacement parameters for X-ray data. The *X*—H bond lengths obtained from the 75 structures were categorized, averaged and compared with the averaged neutron lengths as defined previously (Allen & Bruno, 2010). Additional O—H bonds in water molecules trapped in these structures were also included and the corresponding neutron lengths were taken from Woińska *et. al.* (2016). HAR bond lengths for the 81 structures were taken from Woińska *et al.* (2016). The layout of this figure follows the one proposed in Fig. 2 of the article by Woińska *et al.* (2016). The bars in the figure show the SSDs of each associated bond type.

0.12 Å on average compared to neutron lengths while the difference was an order of magnitude higher than for TAAM results. In the case of co-crystallized water molecules, which were usually disordered, the difference in the mean bond lengths was 0.04 Å with the SSD one third of the neutron SSD.

The precision of determining the X—H bond lengths can be further illustrated by examining the values of SSDs, as proposed by Woinska *et al.* (2016). For NH_2 (NH_2 attached to sp^2 carbon) and O—H bonds (aliphatic, aromatic alcohols and acids) TAAM SSDs were found to be approximately three times larger than neutron SSDs. However, in all these cases the number of observations was less than 30. In all other bond types, the TAAM SSDs were comparable to neutron SSDs (Figs. 1 and S2, Table S2).

While all these comparisons are based on the bond-type classes and may differ in specific individual structures due to the surrounding interactions involved, the disorder in the structures, or the data collection temperature, there was remarkably good agreement between the TAAM and neutron bond lengths.

3.2. Comparison of 0.8 Å resolution X-ray IAM and TAAM refinements with neutron data for averaged *X*—H bond lengths

The issues arising from data collection at high resolution such as lower intensity, merging, trailing of diffraction spots and other experimental errors cannot be ignored. With the aim of using TAAM for routine X-ray data refinement and to estimate accurate and precise X—H bond lengths, we performed TAAM refinement at d_{min} = 0.8 Å by truncating the high-resolution data and comparing the X—H bond lengths with the reference neutron lengths. This comparison is shown in Fig. 1(*b*). The trend remains the same with TAAM results showing the comparable accuracy and precision as at maximum resolution. The difference in individual mean bond lengths varies from 0.001 Å to 0.04 Å compared to neutron bond lengths. However, the differences in mean bond lengths between TAAM and neutron results was significantly reduced for some bond types (Table S2) compared to high-resolution results. This reduction was more prominent in the case of —OH and —NH bonds, irrespective of the number of representatives. For co-crystallized water molecules the difference in mean bond lengths also showed a greater than 50% reduction at 0.8 Å resolution compared to the maximum resolution (Table S2). This reduction in the differences of mean bond lengths at 0.8 Å resolution showed the further improvement in the accuracy of TAAM results with worsening resolution. While TAAM SSDs of most of the bond types improved with data truncation, there were slight increases for —OH and —NH bonds.

The trend of getting even more accurate results with aspherical scattering models when resolution of X-ray diffraction data is artificially truncated was already noted by others (Genoni *et al.*, 2017). This has been explained by the fact that the information content about valence electron redistribution due to chemical bonding, intermolecular polarization and electron correlation is much higher in the low-order reflections than in high-order reflections. Resolution cut-offs change the balance between low-order and high-order reflections contributing to the minimized function, allowing the refinement procedure to achieve more accurate fitting for parameters that are heavily influenced by valence electrons.

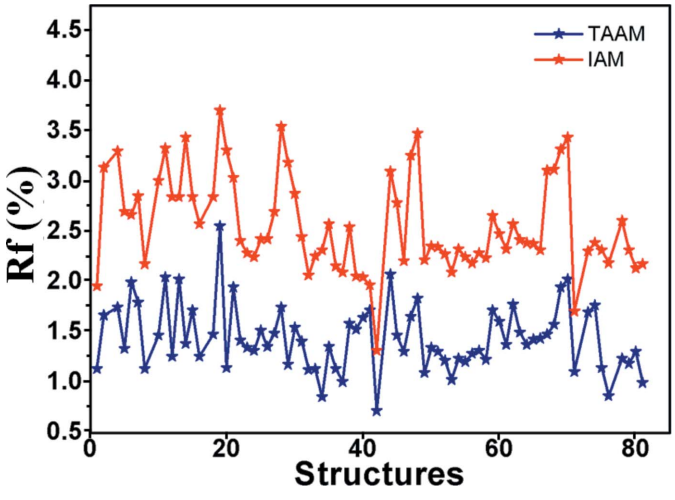

Figure 2
Comparison of reliability factor (R_f) for the TAAM and IAM refinements at 0.8 Å resolution. Hydrogen atoms were refined with isotropic displacement parameters.

3.3. Comparison of other refinement parameters for IAM and TAAM at 0.8 Å resolution

While modeling parameters such as the coordinates of hydrogen atoms from a fit to experimental data, it is important to validate the physical correctness of obtained parameters. Above we showed that TAAM produces more physically

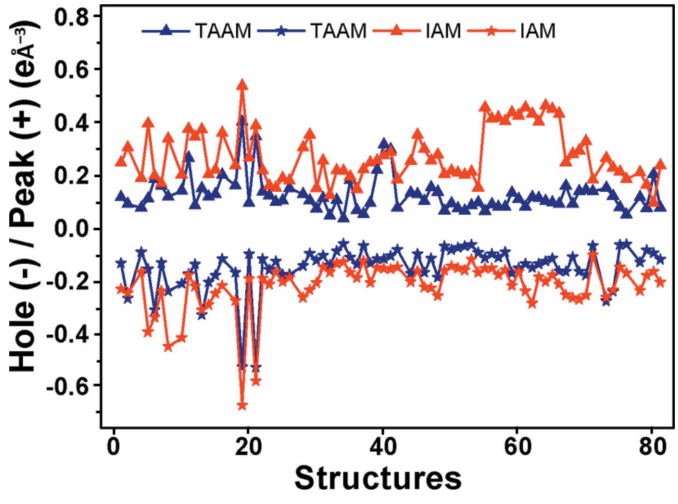

Figure 3
Comparison of residual [*i.e.* peak (+) and hole (−)] electron densities (eÅ^{-3}) for the TAAM and IAM refinement at 0.8 Å resolution. Hydrogen atoms were refined with isotropic displacement parameters. TAAM peak and hole are shown in blue while IAM peak and hole are shown in red.

correct hydrogen atom coordinates than IAM, *i.e.* closer to neutron diffraction data. However, because TAAM was built from the UBDB, the generation of more correct hydrogen-atom coordinates from experimental X-ray data does not prove that TAAM is superior to other methods. UBDB was built from the electron densities of model organic molecules in which hydrogen atoms were positioned at the averaged neutron distances (Dominiak *et al.*, 2007). The fact that the X—H bond lengths from TAAM refinements were closer to neutron diffraction data may only be a result of the 'what you put in is what you get out' effect. This is still acceptable as long as the proposed model not only leads to more physical parameters but also improved fits to experimental data. Here we investigate reliability factors (R_f) [here, $R_1 = \sum ||F_o| - |F_c|| / \sum |F_o|$ with $F_o > 4\sigma(F_o)$] and residual Fourier electron density peaks to show if along with more accurate hydrogen-atom positions the improved fits from TAAM are achieved compared to IAM. In addition, the physical correctness of other fitted parameters such as atomic displacement parameters, should be analyzed. What is measured by an X-ray diffraction experiment is the static crystal electron density distorted by atomic displacements. Atomic displacement parameters may be modified during the least-squares fitting to compensate for weaknesses in the refined model (Gruza *et al.*, 2020). Achieving the proper deconvolution of atomic movements from the electron density is yet another indicator of quality for the electron density model.

The refinement of X-ray data at a standard 0.8 Å resolution with TAAM showed a one percent decrease in the R_f compared to IAM (Fig. 2). However, on one occasion a large value of R_f was observed compared to other structures as seen in Fig. 2 with large blue and red spikes in both IAM and TAAM refinement. A closer look at the structure showed the presence of disorder (structure 19 with CH_3 group disorder). The increase in R_f in the presence of disorder was more prominent in the case of TAAM refinement compared to other non-disordered structures, suggesting that the procedure was more efficient for disorder recognition and possible disorder refinement.

A similar trend was observed in the case of residual (peaks and holes) Fourier electron densities obtained from IAM and TAAM. The residuals from TAAM showed an approximately 0.1 e Å^{-3} decrease compared to IAM as shown in Fig. 3. In a few cases where the disorder was prominent, the residuals were found to be high in the case of TAAM refinement but lower than for IAM. These results further indicate the reliability of TAAM refinement and its sensitivity towards disorder compared to IAM.

We compared the atomic anisotropic displacement parameters (ADPs, here U_{ij}) for non-hydrogen atoms which represent the averaged displacements of atoms from their mean positions in crystals. To find any general trends in the way ADPs from TAAM differ from those from IAM we performed an analysis of the overall size of the displacement ellipsoids by focusing on equivalent isotropic displacement parameters (U_{eq}) computed from U_{ij} (Fischer & Tillmanns, 1988). It appears that TAAM refinement leads to a systematic decrease in non-hydrogen U_{eq} compared to IAM (Fig. 4). TAAM gives comparatively lower values and spread of U_{eq} with respect to IAM in non-disordered structures (Fig. 4). In the case of disordered structures the spread of U_{eq} from TAAM refinement is slightly higher compared to other non-disordered structures but still lower than IAM. Over all structures, the averaged % difference between U_{eq} for non-hydrogen atoms from IAM and from TAAM is 13% (equation 1 in the supporting information).

Further analysis of U_{iso} for hydrogen atoms obtained from IAM and TAAM refinement showed systematically larger values for TAAM compared to IAM (Fig. 5) which is opposite to what had previously been observed in the case of non-hydrogen atoms (Fig. 4). The averaged % difference between U_{iso} of hydrogen atoms obtained from IAM and from TAAM was 32%.

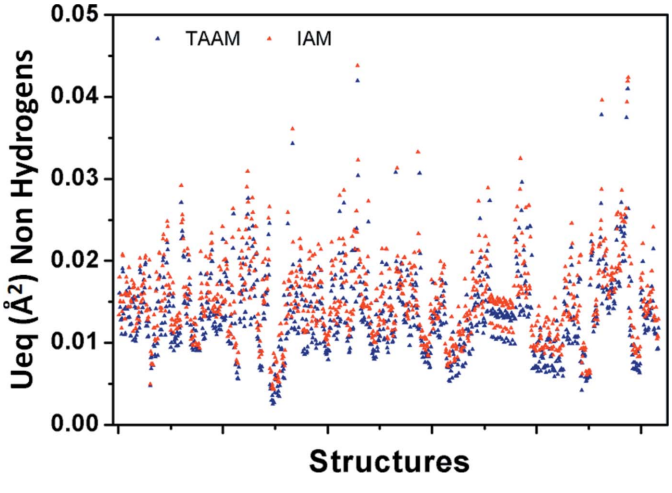

Figure 4
Comparison of U_{eq} (Å^2) for non-hydrogen atoms obtained from TAAM and IAM refinements at 0.8 Å resolution. Hydrogen atoms were refined with isotropic displacement parameters.

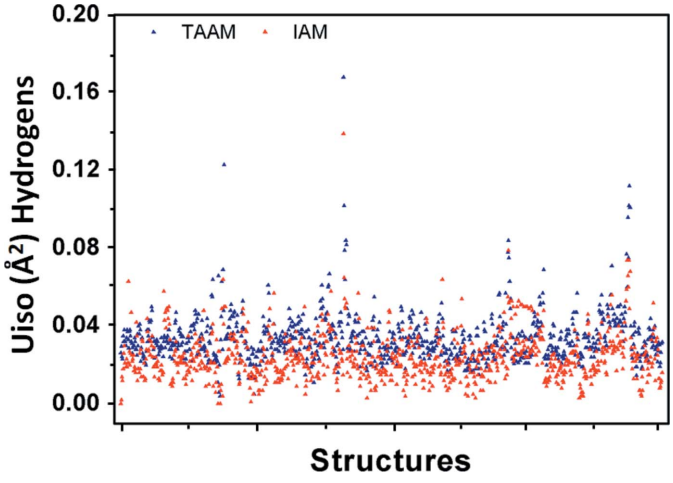

Figure 5
Comparison of U_{iso} (Å^2) for hydrogen atoms obtained from TAAM and IAM refinements at 0.8 Å resolution. Hydrogen atoms were refined with isotropic displacement parameters.

Large scale validation of the U_{eq}/U_{iso} values with neutron data (*i.e.* analogous to the X—H bond length analysis) is much more difficult at the moment as analysis is limited by the amount of atomic displacement parameters available from neutron data. This information was not stored in the CSD and the quality of the available information strongly depends on quality of experimental data (Capelli, Bürgi, Dittrich *et al.*, 2014). Therefore here we decided to focus on selected data sets (23, 24, 49, 80, 81), for which analogous structures from neutron diffraction data that were measured at the same temperatures were available (Capelli, Bürgi, Dittrich *et al.*, 2014; Capelli, Bürgi, Mason & Jayatilaka, 2014; Lübben *et al.*, 2014; Swaminathan *et al.*, 1984; Madsen *et al.*, 2003).

The results are not conclusive. For some structures (Nos. 80 and 81) U_{eq} obtained from TAAM for non-hydrogen atoms were found to be closer to neutron data compared to IAM, for others (Nos. 23, 24 and 49) the opposite is true [Fig. 6(*a*)]. Similar observations for HAR were reported by Capelli, Bürgi, Dittrich *et al.* (2014). In the case of hydrogen atoms, the trend of U_{iso} from TAAM being systematically larger and closer to neutron data than IAM does not seem to depend on the data set and is observed for most of the hydrogen atoms [Fig. 6(*b*)]. The averaged % difference between U_{eq}/U_{iso} for hydrogen atoms obtained from IAM and from neutron data was 50% while the averaged % difference between TAAM and neutron data was only 0.5%.

As reported earlier, ADPs from a conventional spherical atom refinement (IAM) are systematically contaminated by bonding and lone-pair electron densities (Dittrich *et al.*, 2008; Bąk *et al.*, 2011; Domagała *et al.*, 2011). However, validations of ADPs was often compromised by the quality of experimental data (Dittrich *et al.*, 2008; Capelli, Bürgi, Dittrich *et al.*, 2014). Analyses performed not only for high-quality high-resolution experimental X-ray and neutron data but also for simulated X-ray data shed more light on the topic (Gruza *et al.*, 2020). For the simulated data the targeted values of U_{eq}/U_{iso} to be achieved during refinements were predetermined. The U_{eq}/U_{iso} values from TAAM refinements at 0.8 Å were much closer to the target values compared to IAM. Nevertheless, large-scale studies are needed.

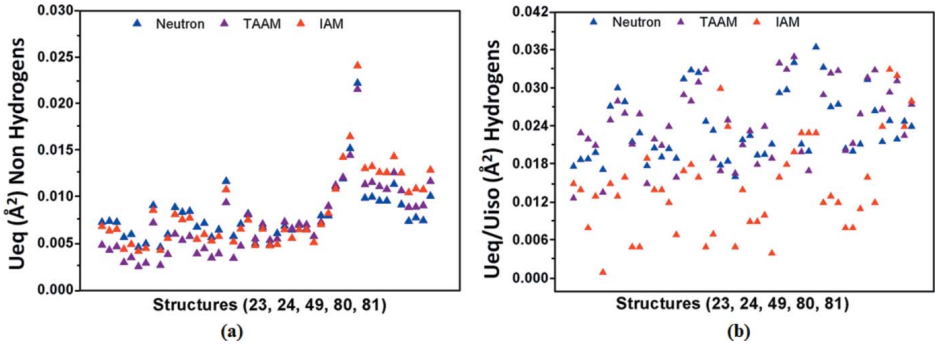

Figure 6
Comparison of U_{eq}/U_{iso} (Å^2) for (*a*) non-hydrogen and (*b*) hydrogen atoms obtained from reported neutron data and IAM and TAAM refinements with X-ray data at 0.8 Å resolution for selected structures (23, 24, 49, 80, 81). Hydrogen atoms were refined with isotropic displacement parameters.

3.4. Comparison of TAAM and HAR results

It is interesting to compare TAAM results to HAR. Before we discuss the results of that comparison, it must be noted that the observed differences do not rely only upon the differences in atomic scattering factors computed either from TAAM or from Hirshfeld atoms. In most of the TAAM refinements we used the reflection data as they were originally published, whereas for HAR, thousands of reflections were omitted from the refinement to achieve convergence. While the general consensus is to use all of the collected intensities in refinement, omission of the weakest intensities sometimes improves the refinement depending upon the method used (*i.e* refinements against $|F|$ or F^2) (Merli, 2002). Moreover, there are many more differences between our TAAM refinements and published HAR; data were refined against structure factor magnitudes $|F|$ (HAR) or F^2 (TAAM) and the weighting schemes were different. Only when the same refinement strategy with the same software implementation is used, the effects of replacing TAAM scattering factors by Hirshfeld atoms can been investigated more deeply.

The values obtained for the averaged X—H bond lengths from TAAM are within the same magnitude range as those of HAR bond lengths, though HAR results are systematically slightly closer to neutron data than TAAM (Fig. 1). For refinements at 0.8 Å resolution with isotropic hydrogen displacement parameters, the mean TAAM bond lengths averaged over all bond types were shorter by 0.020 Å compared to neutron lengths whereas the averaged shortening for HAR was 0.014 Å. The importance of the difference might be further judged from the SSDs of TAAM and HAR results, which were compared by plotting the difference between the TAAM and HAR mean bond lengths along with HAR and TAAM SSDs (Fig. S3). The SSDs from TAAM are comparable to HAR in most cases and in the remaining cases they were either higher (mostly bond types belonging to Z—O—H and Z—Csp^3—H$_3$ groups) or lower than the HAR SSDs. Only on a few occasions was the mean X—H bond length difference between TAAM and HAR larger than one SSD.

The refinement indicators at standard 0.8 Å resolution such as R_f and residual densities from TAAM were also comparable to HAR (Figs. S4 and S5). In most cases the differences in HAR and TAAM indicators were much smaller than the differences between any of these two methods and IAM, although the HAR results usually were slightly better. The U_{eq} parameters for non-hydrogen atoms from HAR were comparable to TAAM, the averaged percentage difference between TAAM and HAR U_{eq} was found to be 0.8% (Fig. S6). For hydrogen atoms the averaged percentage difference between TAAM and HAR U_{iso} was found to be 7% (Fig. S7). Further studies are

needed to investigate which method, HAR or TAAM, gives U_{eq}/U_{iso} closer to reality.

Even more detailed comparison between HAR and TAAM refinement was performed on four structures (27, 36, 42, 75) where the reflections were removed as was done in the case of HAR. Here results for both refinement resolutions (maximum or 0.8 Å) as well as both types of hydrogen-atom displacements (isotropic or anisotropic) were analyzed. In all cases, the refinement parameters (R_f, residual densities) and U_{eq} for non-hydrogen atoms thus obtained from TAAM were very similar to HAR (Table S3, Fig. S8).

3.5. Anisotropic refinement of hydrogen-atom displacements using TAAM approach

It was long believed that it was not possible to obtain reliable anisotropic displacement parameters for hydrogen atoms directly from standard X-ray diffraction data. There are various tools available for estimation of hydrogen ADPs. These are, for example, the segmented-body translation libration screw (TLS) refinement method along with Invariom approach used in the *ADP-toolkit* program (Lübben *et al.*, 2015), or the SHADE method using ADPs from neutron experiments to approximate hydrogen ADPs and available from the *SHADE* web server (Madsen *et al.*, 2003; Madsen & Hoser, 2014). It was also shown that for sub-atomic resolution X-ray data of exceptional quality, the multipolar model with polarized hydrogen atoms and additional bond-directed dipoles also lead to hydrogen ADPs close to the neutron values (Zhurov *et al.*, 2011). Refinements of hydrogen ADPs with X-ray data using the HAR method livened-up the discussion, as the authors proposed that HAR may give reliable hydrogen ADPs (Jayatilaka & Dittrich, 2008; Capelli, Bürgi, Dittrich *et al.*, 2014). A recent comparison of different strategies in modeling the hydrogen atoms indicates that although HAR yields reliable C—H bond lengths, caution should be taken if hydrogen ADPs are to be obtained with this method (Köhler *et al.*, 2019).

To provide more results to the discussion we decided to check if it is possible to routinely obtain hydrogen ADPs from TAAM refinements with X-ray data and how obtained parameters compare with other methods. Anisotropic refinements of hydrogen atoms were performed on 75 structures using TAAM. In most cases hydrogen ADPs were successfully refined. Successful refinements were those that were stable and convergence was achieved, and non-positive definite (NPD) ADPs were not observed or observed for only one or two atoms per structure. Statistical analyses analogous to the one above for isotropic refinements were also performed. The averaged X—H bond lengths were comparable to averaged neutron bond lengths (Fig. S9); however, noticeable changes were visible compared to isotropic hydrogen refinement. The averaged X—H bond lengths improved in some cases but not others (Fig. S10), which was consistent with a similar observation for HAR (Woińska *et al.*, 2016). There were marginal to significant improvements in R_f and residuals in anisotropic hydrogen refinement compared to isotropic hydrogen refinement at 0.8 Å resolution (Figs. S11 and S12). The refinement parameters obtained from TAAM were also comparable to the HAR results at 0.8 Å resolution (Figs. S13 and S14). The hydrogen ADPs were obtained from information derived from the X-ray data for a particular compound and hence the quality of the ADPs is poor in some cases, more often with obliqueness and oblateness. Out of all the anisotropically refined hydrogen atoms (949) only 4% (41) were found to be showing NPD at 0.8 Å resolution and 1% (10) at maximum reported resolution, which is consistent with the HAR results (Woińska *et al.*, 2016). The NPDs were found mostly in those cases where the water molecules were disordered or the data quality was poor.

In order to further investigate and verify the correctness of the hydrogen ADPs, comparisons were drawn between the hydrogen U_{ij} values obtained from neutron, HAR and TAAM refinements, respectively, at 0.8 Å resolution, made for five representative crystal structures, Nos. 23, 24, 49, 80 and 81. A comparison for U_{ij} values shows a good correlation ($R^2 = 0.70$) between TAAM and neutron U_{ij} values which was comparable to the correlation between neutron and HAR ($R^2 = 0.78$) (Fig. S15). The correlation coefficient between TAAM and HAR U_{ij} was found to be 0.87. A negligible change in the correlation coefficient was observed when the data with the omitted reflections were used (Fig. S15). Further we compared the ADPs (U_{ij}) for all the atoms from structures 23, 24, 49, 80 and 81 using similarity index (S_{12}) (Whitten & Spackman, 2006). For two ADP tensors, the lower the S_{12} value was, the higher the observed similarity was, $S_{12} = 0$ means that these two tensors were exactly the same. We observed (Table S4) that TAAM ADPs for non-hydrogen atoms showed similarity (S_{12}) with neutron ADPs comparable to the HAR results reported by Woińska *et al.* (2016), and this was true for all five structures and both versions of refinements (with or without omissions of reflections in TAAM). For hydrogen ADPs, ignoring the NPDs, similarity indexes obtained for TAAM and HAR were also somewhat comparable.

4. Conclusions

In conclusion, we have confirmed the high accuracy and precision of mean X—H bond lengths obtained from TAAM, which were comparable to the mean neutron bond lengths, both at the maximum reported and 0.8 Å resolution. At 0.8 Å resolution the accuracy further improved compared to high resolution, especially in the case of the polar hydrogen atoms in NH and OH bond types. The TAAM refinement showed sensitivity towards disorder with high values of refinement parameter indicators. A comparison at 0.8 Å resolution between the IAM and TAAM refinement showed a significant improvement in refinement parameter indicators such as R_f values and residual electron densities for TAAM. A systematic and significant reduction in displacement parameters for non-hydrogen atoms and enlargement for hydrogen atoms was observed in TAAM refinements at 0.8 Å compared to IAM. Limited comparisons to neutron data suggested that atomic displacements for hydrogen atoms from

TAAM were physically more meaningful than from IAM; further studies are needed to validate non-hydrogen-atom displacement parameters. The comparison of refinement parameter indicators for TAAM and HAR showed good agreement. All the results showed that the accuracy and precision of X—H bond lengths from TAAM refinement were not much worse than those reported from HAR and the obtained bond lengths were not worse than the reference neutron bond distances. It was indeed possible to refine hydrogen displacement parameters anisotropically using TAAM with good quality X-ray data and the results obtained were satisfactorily close to neutron values. Introduction of anisotropic hydrogen atoms did not appear to improve the other refinement parameters; further studies are need to confirm that the procedure does not cause overfitting.

These encouraging results establish the usefulness of TAAM for routine structure determination using X-ray data which is accessible to scientific users interested in the study of hydrogen bonds. TAAM refinements localize hydrogen atoms almost as accurately and precisely as neutron diffraction, overcoming deficiencies of IAM, as showed by bond lengths and displacement parameters. Moreover, the integration of TAAM methodology with *Olex2*, which is available for structure refinement to the crystallography community, makes TAAM a reliable and user-friendly tool to be applied in the last steps of refinement during routine X-ray structure determination of organic molecule crystals. Application of TAAM to polymer network structures, disordered compounds (Bąk *et al.*, 2009; Dittrich *et al.*, 2016), organic fragments in organometallic complexes (Wandtke *et al.*, 2017) or molecular biology (Jelsch *et al.*, 1998; Malinska & Dauter, 2016) seems to be possible and it will be investigated in future works. General applicability of TAAM from a databank for metal atoms and inorganic structures is currently not possible with the existing atom-typing algorithm and multipolar model parametrization used to build the databank, and requires further feasibility studies. Another missing feature of the current TAAM implementation is a lack of crystal field effects in the model built from UBDB, which in the future may possibly be overcome by implementation of the ELMAM2 database.

5. Related literature

The following references are cited in the supporting information: Munshi *et al.* (2006); Zarychta *et al.* (2011); Chen *et al.* (2007); Nassour *et al.* (2014); Slouf *et al.* (2002); Munshi & Guru Row (2002, 2006); Bianchi *et al.* (1998); Janicki & Starynowicz (2010); Bürgi *et al.* (2002); Zhurova & Pinkerton (2001); Małecka *et al.* (2010); Dittrich *et al.* (2009, 2002, 2012, 2007); Meents *et al.* (2008); Bibila Mayaya Bisseyou *et al.* (2012); Gulliot *et al.* (2001); Flaig *et al.* (1998, 1999); Tsirelson *et al.* (2006); Farrugia *et al.* (2002); Pichon-Pesme *et al.* (2000); Benabicha *et al.* (2000); Śled *et al.* (2010); Chęcińska *et al.* (2011, 2006); Förster *et al.* (2005); Grabowsky *et al.* (2005); Kalinowski *et al.* (2007); Scheins *et al.* (2004, 2005); Lübben *et al.* (2014); Dahaoui *et al.* (1999); Kamiński *et al.* (2014); Paul *et al.* (2011); Poulain *et al.* (2014); Zhurova *et al.* (2006); Holstein *et al.* (2010); Dittrich & Spackman (2007); Jaradat *et al.* (2007); Hübschle *et al.* (2008); Birkedal *et al.* (2004).

Acknowledgements

MLC thanks Luc Bourhis, Oleg Dolomanov and Horst Puschmann for information/comments on integration of *DiSCaMB* functionality into *Olex2*. KKJ thanks Magdalena Woińska for disclosing all the methodological details regarding the work presented by Woińska *et al.* (2016).

Funding information

The following funding is acknowledged: the National Centre of Science (Poland) (grant OPUS No. UMO-2017/27/B/ST4/02721 to Paulina Maria Dominiak) and PL-Grid Infrastructure through grant UBDB2019.

References

Agback, P. & Agback, T. (2018). *Sci. Rep.* **8**, 1–6.
Ahmed, M., Noureen, S., Gros, P. C., Guillot, B. & Jelsch, C. (2011). *Acta Cryst.* C**67**, o329–o333.
Allen, F. H. & Bruno, I. J. (2010). *Acta Cryst.* B**66**, 380–386.
Almlöf, J. & Ottersen, T. (1979). *Acta Cryst.* A**35**, 137–139.
Bąk, J. M., Domagała, S., Hübschle, C., Jelsch, C., Dittrich, B. & Dominiak, P. M. (2011). *Acta Cryst.* A**67**, 141–153.
Bąk, J. M., Dominiak, P. M., Wilson, C. C. & Woźniak, K. (2009). *Acta Cryst.* A**65**, 490–500.
Belkova, N. V., Epstein, L. M., Filippov, O. A. & Shubina, E. S. (2016). *Chem. Rev.* **116**, 8545–8587.
Benabicha, F., Pichon-Pesme, V., Jelsch, C., Lecomte, C. & Khmou, A. (2000). *Acta Cryst.* B**56**, 155–165.
Bendeif, E. & Jelsch, C. (2007). *Acta Cryst.* C**63**, o361–o364.
Bianchi, R., Gervasio, G. & Viscardi, G. (1998). *Acta Cryst.* B**54**, 66–72.
Bibila Mayaya Bisseyou, Y., Bouhmaida, N., Guillot, B., Lecomte, C., Lugan, N., Ghermani, N. & Jelsch, C. (2012). *Acta Cryst.* B**68**, 646–660.
Birkedal, H., Madsen, D., Mathiesen, R. H., Knudsen, K., Weber, H.-P., Pattison, P. & Schwarzenbach, D. (2004). *Acta Cryst.* A**60**, 371–381.
Brock, C. P., Dunitz, J. D. & Hirshfeld, F. L. (1991). *Acta Cryst.* B**47**, 789–797.
Bürgi, H.-B., Capelli, S. C., Goeta, A. E., Howard, J. A. K., Spackman, M. A. & Yufit, D. S. (2002). *Chem. Eur. J.* **8**, 3512–3521.
Capelli, S. C., Bürgi, H.-B., Dittrich, B., Grabowsky, S. & Jayatilaka, D. (2014). *IUCrJ*, **1**, 361–379.
Capelli, S. C., Bürgi, H.-B., Mason, S. A. & Jayatilaka, D. (2014). *Acta Cryst.* C**70**, 949–952.
Chęcińska, L., Förster, D., Morgenroth, W. & Luger, P. (2006). *Acta Cryst.* C**62**, o454–o457.
Chęcińska, L., Grabowsky, S., Małecka, M., Rybarczyk-Pirek, A. J., Jóźwiak, A., Paulmann, C. & Luger, P. (2011). *Acta Cryst.* B**67**, 569–581.
Chen, D., Oezguen, N., Urvil, P., Ferguson, C., Dann, S. M. & Savidge, T. C. (2016). *Sci. Adv.* **2**, e1501240.
Chen, Y.-S., Stash, A. I. & Pinkerton, A. A. (2007). *Acta Cryst.* B**63**, 309–318.
Chodkiewicz, M. L., Migacz, S., Rudnicki, W., Makal, A., Kalinowski, J. A., Moriarty, N. W., Grosse-Kunstleve, R. W., Afonine, P. V., Adams, P. D. & Dominiak, P. M. (2018). *J. Appl. Cryst.* **51**, 193–199.
Coppens, P. (1968). *Acta Cryst.* B**24**, 1272–1274.

Coppens, P. (1997). *X-ray Charge Densities and Chemical Bonding*. International Union of Crystallography and Oxford University Press.

Dadda, N., Nassour, A., Guillot, B., Benali-Cherif, N. & Jelsch, C. (2012). *Acta Cryst.* A**68**, 452–463.

Dahaoui, S., Jelsch, C., Howard, J. A. K. & Lecomte, C. (1999). *Acta Cryst.* B**55**, 226–230.

Destro, R., Marsh, R. E. & Bianchi, R. (1988). *J. Phys. Chem.* **92**, 966–973.

Destro, R., Roversi, P., Barzaghi, M. & Marsh, R. E. (2000). *J. Phys. Chem. A*, **104**, 1047–1054.

Dittrich, B., Hübschle, C. B., Holstein, J. J. & Fabbiani, F. P. A. (2009). *J. Appl. Cryst.* **42**, 1110–1121.

Dittrich, B., Hübschle, C. B., Messerschmidt, M., Kalinowski, R., Girnt, D. & Luger, P. (2005). *Acta Cryst.* A**61**, 314–320.

Dittrich, B., Hübschle, C. B., Pröpper, K., Dietrich, F., Stolper, T. & Holstein, J. (2013). *Acta Cryst.* B**69**, 91–104.

Dittrich, B., Koritsánszky, T., Grosche, M., Scherer, W., Flaig, R., Wagner, A., Krane, H. G., Kessler, H., Riemer, C., Schreurs, A. M. M. & Luger, P. (2002). *Acta Cryst.* B**58**, 721–727.

Dittrich, B., Koritsánszky, T. & Luger, P. (2004). *Angew. Chem. Int. Ed.* **43**, 2718–2721.

Dittrich, B., Lübben, J., Mebs, S., Wagner, A., Luger, P. & Flaig, R. (2017). *Chem. Eur. J.* **23**, 4605–4614.

Dittrich, B., McKinnon, J. J. & Warren, J. E. (2008). *Acta Cryst.* B**64**, 750–759.

Dittrich, B., Munshi, P. & Spackman, M. A. (2006). *Acta Cryst.* C**62**, o633–o635.

Dittrich, B., Munshi, P. & Spackman, M. A. (2007). *Acta Cryst.* B**63**, 505–509.

Dittrich, B., Schürmann, C. & Hübschle, C. B. (2016). *Z. Kristallogr.* **231**, 725–736.

Dittrich, B. & Spackman, M. A. (2007). *Acta Cryst.* A**63**, 426–436.

Dittrich, B., Sze, E., Holstein, J. J., Hübschle, C. B. & Jayatilaka, D. (2012). *Acta Cryst.* A**68**, 435–442.

Dittrich, B., Hübschle, C. B., Luger, P. & Spackman, M. A. (2006). *Acta Cryst.* D**62**, 1325–1335.

Dolomanov, O. V., Bourhis, L. J., Gildea, R. J., Howard, J. A. K. & Puschmann, H. (2009). *J. Appl. Cryst.* **42**, 339–341.

Domagała, S., Fournier, B., Liebschner, D., Guillot, B. & Jelsch, C. (2012). *Acta Cryst.* A**68**, 337–351.

Domagała, S., Munshi, P., Ahmed, M., Guillot, B. & Jelsch, C. (2011). *Acta Cryst.* B**67**, 63–78.

Dominiak, P. M., Volkov, A., Li, X., Messerschmidt, M. & Coppens, P. (2007). *J. Chem. Theory Comput.* **3**, 232–247.

Doyle, A. G. & Jacobsen, E. N. (2007). *Chem. Rev.* **107**, 5713–5743.

Emsley, J. (2011). *Nature's Building Blocks: an A–Z Guide to the Elements*. Oxford University Press.

Farrugia, L. J., Kočovský, P., Senn, H. M. & Vyskočil, S. (2009). *Acta Cryst.* B**65**, 757–769.

Fischer, R. X. & Tillmanns, E. (1988). *Acta Cryst.* C**44**, 775–776.

Flaig, R., Koritsánszky, T., Janczak, J., Krane, H.-G., Morgenroth, W. & Luger, P. (1999). *Angew. Chem. Int. Ed.* **38**, 1397–1400.

Flaig, R., Koritsanszky, T., Zobel, D. & Luger, P. (1998). *J. Am. Chem. Soc.* **120**, 2227–2238.

Förster, D., Messerschmidt, M. & Luger, P. L. (2005). *Acta Cryst.* C**61**, o420–o421.

Fugel, M., Jayatilaka, D., Hupf, E., Overgaard, J., Hathwar, V. R., Macchi, P., Turner, M. J., Howard, J. A. K., Dolomanov, O. V., Puschmann, H., Iversen, B. B., Bürgi, H.-B. & Grabowsky, S. (2018). *IUCrJ*, **5**, 32–44.

Genoni, A., Dos Santos, L. H. R., Meyer, B. & Macchi, P. (2017). *IUCrJ*, **4**, 136–146.

Gildea, R. J., Bourhis, L. J., Dolomanov, O. V., Grosse-Kunstleve, R. W., Puschmann, H., Adams, P. D. & Howard, J. A. K. (2011). *J. Appl. Cryst.* **44**, 1259–1263.

Głowacki, E. D., Irimia-Vladu, M., Bauer, S. & Sariciftci, N. S. (2013). *J. Mater. Chem. B*, **1**, 3742–3753.

Grabowsky, S., Kalinowski, R., Weber, M., Förster, D., Paulmann, C. & Luger, P. (2009). *Acta Cryst.* B**65**, 488–501.

Groom, C. R., Bruno, I. J., Lightfoot, M. P. & Ward, S. C. (2016). *Acta Cryst.* B**72**, 171–179.

Gruza, B., Chodkiewicz, M. L., Krzeszczakowska, J. & Dominiak, P. M. (2020). *Acta Cryst.* A**76**, 92–109.

Guillot, R., Muzet, N., Dahaoui, S., Lecomte, C. & Jelsch, C. (2001). *Acta Cryst.* B**57**, 567–578.

Hansen, N. K. & Coppens, P. (1978). *Acta Cryst.* A**34**, 909–921.

Hirshfeld, F. L. (1977). *Theor. Chim. Acta*, **44**, 129–138.

Holstein, J. J., Luger, P., Kalinowski, R., Mebs, S., Paulman, C. & Dittrich, B. (2010). *Acta Cryst.* B**66**, 568–577.

Hope, H. & Ottersen, T. (1978). *Acta Cryst.* B**34**, 3623–3626.

Hoser, A. A., Dominiak, P. M. & Woźniak, K. (2009). *Acta Cryst.* A**65**, 300–311.

Hübschle, C. B., Dittrich, B., Grabowsky, S., Messerschmidt, M. & Luger, P. (2008). *Acta Cryst.* B**64**, 363–374.

Janicki, R. & Starynowicz, P. (2010). *Acta Cryst.* B**66**, 559–567.

Jaradat, D. M. M., Mebs, S., Chęcińska, L. & Luger, P. (2007). *Carbohydr. Res.* **342**, 1480–1489.

Jarzembska, K. N. & Dominiak, P. M. (2012). *Acta Cryst.* A**68**, 139–147.

Jayatilaka, D. & Dittrich, B. (2008). *Acta Cryst.* A**64**, 383–393.

Jayatilaka, D. & Grimwood, D. J. (2003). *Computational Science – ICCS 2003*, edited by P. M. A. Sloot, D. Abramson, A. V. Bogdanov, Y. E. Gorbachev, J. J. Dongarra and A. Y. Zomaya, pp. 142–151. Berlin, Heidelberg: Springer.

Jelsch, C., Pichon-Pesme, V., Lecomte, C. & Aubry, A. (1998). *Acta Cryst.* D**54**, 1306–1318.

Kalinowski, R., Dittrich, B., Hübschle, C. B., Paulmann, C. & Luger, P. (2007). *Acta Cryst.* B**63**, 753–767.

Kamiński, R., Domagała, S., Jarzembska, K. N., Hoser, A. A., Sanjuan-Szklarz, W. F., Gutmann, M. J., Makal, A., Malińska, M., Bąk, J. M. & Woźniak, K. (2014). *Acta Cryst.* A**70**, 72–91.

Köhler, C., Lübben, J., Krause, L., Hoffmann, C., Herbst-Irmer, R. & Stalke, D. (2019). *Acta Cryst.* B**75**, 434–441.

Kumar, P., Gruza, B., Bojarowski, S. A. & Dominiak, P. M. (2019). *Acta Cryst.* A**75**, 398–408.

Lübben, J., Bourhis, L. J. & Dittrich, B. (2015). *J. Appl. Cryst.* **48**, 1785–1793.

Lübben, J., Volkmann, C., Grabowsky, S., Edwards, A., Morgenroth, W., Fabbiani, F. P. A., Sheldrick, G. M. & Dittrich, B. (2014). *Acta Cryst.* A**70**, 309–316.

Lübben, J., Wandtke, C. M., Hübschle, C. B., Ruf, M., Sheldrick, G. M. & Dittrich, B. (2019). *Acta Cryst.* A**75**, 50–62.

Madsen, A. Ø. & Hoser, A. A. (2014). *J. Appl. Cryst.* **47**, 2100–2104.

Madsen, A. Ø., Mason, S. & Larsen, S. (2003). *Acta Cryst.* B**59**, 653–663.

Madsen, A. Ø., Sørensen, H. O., Flensburg, C., Stewart, R. F. & Larsen, S. (2004). *Acta Cryst.* A**60**, 550–561.

Malaspina, L. A., Wieduwilt, E. K., Bergmann, J., Kleemiss, F., Meyer, B., Ruiz-López, M. F., Pal, R., Hupf, E., Beckmann, J., Piltz, R. O., Edwards, A. J., Grabowsky, S. & Genoni, A. (2019). *J. Phys. Chem. Lett.* **10**, 6973–6982.

Małecka, M., Chęcińska, L., Rybarczyk-Pirek, A., Morgenroth, W. & Paulmann, C. (2010). *Acta Cryst.* B**66**, 687–695.

Malinska, M. & Dauter, Z. (2016). *Acta Cryst.* D**72**, 770–779.

Meents, A., Dittrich, B., Johnas, S. K. J., Thome, V. & Weckert, E. F. (2008). *Acta Cryst.* B**64**, 42–49.

Merli, M. (2002). *Z. Kristallogr.* **217**, 103–108.

Meyer, B. & Genoni, A. (2018). *J. Phys. Chem. A*, **122**, 8965–8981.

Meyer, B., Guillot, B., Ruiz-Lopez, M. F. & Genoni, A. (2016). *J. Chem. Theory Comput.* **12**, 1052–1067.

Midgley, L., Bourhis, L. J., Dolomanov, O., Peyerimhoff, N. & Puschmann, H. (2019). arXiv: 1911.08847.

Müller, P., Herbst-Irmer, R., Spek, A. L., Schneider, T. R. & Sawaya, M. R. (2006). *Crystal Structure Refinement: A Crystallographer's Guide to SHELXL*. Oxford University Press.

Munshi, P. & Guru Row, T. N. (2002). *Acta Cryst.* B**58**, 1011–1017.
Munshi, P. & Guru Row, T. N. (2006). *Acta Cryst.* B**62**, 612–626.
Munshi, P., Thakur, T. S., Guru Row, T. N. & Desiraju, G. R. (2006). *Acta Cryst.* B**62**, 118–127.
Nassour, A., Domagala, S., Guillot, B., Leduc, T., Lecomte, C. & Jelsch, C. (2017). *Acta Cryst.* B**73**, 610–625.
Nassour, A., Kubicki, M., Wright, J., Borowiak, T., Dutkiewicz, G., Lecomte, C. & Jelsch, C. (2014). *Acta Cryst.* B**70**, 197–211.
Overgaard, J., Platts, J. A. & Iversen, B. B. (2009). *Acta Cryst.* B**65**, 715–723.
Paul, A., Kubicki, M., Jelsch, C., Durand, P. & Lecomte, C. (2011). *Acta Cryst.* B**67**, 365–378.
Petříček, V., Dušek, M. & Palatinus, L. (2014). *Z. Kristallogr. Mater.* **229**, 345–352.
Pichon-Pesme, V., Jelsch, C., Guillot, B. & Lecomte, C. (2004). *Acta Cryst.* A**60**, 204–208.
Pichon-Pesme, V., Lachekar, H., Souhassou, M. & Lecomte, C. (2000). *Acta Cryst.* B**56**, 728–737.
Poulain, A., Wenger, E., Durand, P., Jarzembska, K. N., Kamiński, R., Fertey, P., Kubicki, M. & Lecomte, C. (2014). *IUCrJ*, **1**, 110–118.
Roversi, P., Merati, F., Destro, R. & Barzaghi, M. (1996). *Can. J. Chem.* **74**, 1145–1161.
Ruysink, A. F. J. & Vos, A. (1974). *Acta Cryst.* A**30**, 503–506.
Scheins, S., Dittrich, B., Messerschmidt, M., Paulmann, C. & Luger, P. (2004). *Acta Cryst.* B**60**, 184–190.
Scheins, S., Messerschmidt, M. & Luger, P. (2005). *Acta Cryst.* B**61**, 443–448.
Sheldrick, G. M. (2015). *Acta Cryst.* C**71**, 3–8.
Śledź, P., Kamiński, R., Chruszcz, M., Zimmerman, M. D., Minor, W. & Woźniak, K. (2010). *Acta Cryst.* B**66**, 482–492.
Slouf, M., Holy, A., Petříček, V. & Cisarova, I. (2002). *Acta Cryst.* B**58**, 519–529.
Spek, A. L. (2003). *J. Appl. Cryst.* **36**, 7–13.
Spek, A. L. (2020). *Acta Cryst.* E**76**, 1–11.
Stalke, D. (2012). *Electron Density and Chemical Bonding I: Experimental Charge Density Studies*. Springer.
Stewart, R. F., Bentley, J. & Goodman, B. (1975). *J. Chem. Phys.* **63**, 3786–3793.
Stewart, R. F., Davidson, E. R. & Simpson, W. T. (1965). *J. Chem. Phys.* **42**, 3175–3187.
Swaminathan, S., Craven, B. M. & McMullan, R. K. (1984). *Acta Cryst.* B**40**, 300–306.
Taylor, M. S. & Jacobsen, E. N. (2006). *Angew. Chem. Int. Ed.* **45**, 1520–1543.
Tsirelson, V. G., Stash, A. I., Potemkin, V. A., Rykounov, A. A., Shutalev, A. D., Zhurova, E. A., Zhurov, V. V., Pinkerton, A. A., Gurskaya, G. V. & Zavodnik, V. E. (2006). *Acta Cryst.* B**62**, 676–688.
Vladilo, G. & Hassanali, A. (2018). *Life*, **8**, 1–22.
Volkov, A., Li, X., Koritsanszky, T. & Coppens, P. (2004). *J. Phys. Chem. A*, **108**, 4283–4300.
Volkov, A., Macchi, P., Farrugia, L. J., Gatti, C., Mallinson, P., Richter, T. & Koritsanszky, T. (2006). *XD2006.* University at Buffalo, NY, USA, University of Milan, Italy, University of Glasgow, UK, CNRISTM, Milan, Italy, and Middle Tennessee State University, TN, USA.
Volkov, A., Messerschmidt, M. & Coppens, P. (2007). *Acta Cryst.* D**63**, 160–170.
Wandtke, C. M., Weil, M., Simpson, J. & Dittrich, B. (2017). *Acta Cryst.* B**73**, 794–804.
Whitten, A. E. & Spackman, M. A. (2006). *Acta Cryst.* B**62**, 875–888.
Wilson, A. J. C. & Geist, V. (1993). *Cryst. Res. Technol.* **28**, 110.
Woińska, M., Grabowsky, S., Dominiak, P. M., Woźniak, K. & Jayatilaka, D. (2016). *Sci. Adv.* **2**, e1600192.
Woińska, M., Jayatilaka, D., Spackman, M. A., Edwards, A. J., Dominiak, P. M., Woźniak, K., Nishibori, E., Sugimoto, K. & Grabowsky, S. (2014). *Acta Cryst.* A**70**, 483–498.
Zarychta, B., Pichon-Pesme, V., Guillot, B., Lecomte, C. & Jelsch, C. (2007). *Acta Cryst.* A**63**, 108–125.
Zarychta, B., Zaleski, J., Kyzioł, J., Daszkiewicz, Z. & Jelsch, C. (2011). *Acta Cryst.* B**67**, 250–262.
Zhurova, E. A. & Pinkerton, A. A. (2001). *Acta Cryst.* B**57**, 359–365.
Zhurova, E. A., Tsirelson, V. G., Zhurov, V. V., Stash, A. I. & Pinkerton, A. A. (2006). *Acta Cryst.* B**62**, 513–520.
Zhurov, V. V., Zhurova, E. A., Stash, A. I. & Pinkerton, A. A. (2011). *Acta Cryst.* A**67**, 160–173.